

Regular article

Modeling the H_5^+ potential-energy surface: a first attempt

Rita Prosmi¹, Alexei A. Buchachenko^{1,2}, Pablo Villarreal¹, Gerardo Delgado-Barrio¹

¹Instituto de Matemáticas y Física Fundamental, C.S.I.C., Serrano 123, 28006 Madrid, Spain

²Department of Chemistry, Moscow State University, Moscow 119899, Russia

Received: 15 March 2001 / Accepted: 5 July 2001 / Published online: 11 October 2001

© Springer-Verlag 2001

Abstract. Ab initio molecular electronic structure calculations are performed for H_5^+ at the QCISD(T) level of theory, using a correlation-consistent quadruple-zeta basis set. Structures, vibrational frequencies and thermochemical properties are evaluated for ten stationary points of the H_5^+ hypersurface and are compared with previous calculations. The features of the $H_3^+ \dots H_2$ interaction at intermediate and large intermolecular distances are also investigated. Furthermore, an analytical functional form for the potential-energy surface of H_5^+ is derived using a first-order diatomics-in-molecule perturbation theory approach. Its topology is found to be qualitatively correct for the short-range interaction region.

Key words: Ab initio calculations – Potential-energy surface – Ionic clusters

1 Introduction

Positively charged hydrogen clusters $H_3^+ \cdot (H_2)_n$ represent one of the most simple and interesting examples of the heterogeneous weakly-bound ion-molecular aggregates suitable for modeling the nucleation dynamics in stratospheric or interstellar conditions and for understanding the solvation mechanisms in liquids.

Since the detection of the first member of the series, H_3^+ , in 1962 [1], many experimental studies of dissociation energies and thermochemical properties of the H_n^+ clusters have been performed (reviewed in Refs. [2–4]). One of the most detailed experimental studies was carried out by Okumura et al. [2], using IR vibrational predissociation spectroscopy. They observed the vibrational frequencies of H_2 and H_3^+ in $H_3^+ \cdot (H_2)_n$ ionic clusters for $n=1-6$ and they analyzed the dependence of the shift of these vibrations with the size of the cluster. Numerous ab initio calculations have been carried out

[3–8] aiming to determine their equilibrium structures, low-lying stationary points and dissociation energies. A very detailed ab initio investigation of the H_5^+ cluster was carried out by Yamaguchi et al. [3]. They revealed a quite complicated structure of the interaction potential: ten distinct stationary points were located and analyzed at ten different levels of theory. Their high-level calculations predicted a C_{2v} structure as the only minimum. Currently, equilibrium structures and energetics of H_5^+ and larger clusters remain a topic of intense attention [9, 10]. In these studies calculations were carried out at the MP2/MP4, CCSD(T) and G2(MP2) levels of theory using the 6-311G** basis set, in order to investigate the shell structures and magic numbers in the stabilization energy for $H_3^+(H_2)_n$, ($n=1-9$) clusters.

A more complicated and demanding theoretical task is the construction of the global potential-energy surfaces (PESs) of H_5^+ and larger clusters. They are needed in order to use H_n^+ clusters as prototypes to explore gas-phase solvation processes and to interpret various experimental data on the dynamics of cluster fragmentation [2, 11] and $H_3^+ + H_2$ collisions [5, 12]. To our knowledge, few attempts in this direction have been performed so far. Ahlrichs [5], using PNO-CI and CEPA methods, found the D_{2d} structure to present the absolute minimum on the H_5^+ surface. Further, he analyzed the flatness of the PES in the vicinity of the D_{2d} configuration and the mobility of the central proton. By calculating the Hartree–Fock interaction energies of isomeric H_5^+ structures, he also investigated the long-range behavior of its PES. Nagashima et al. [4] described the intermolecular $H_3^+ - H_2$ potential (at frozen configuration of the fragments) by a sum of site–site interactions that was fitted to ab initio calculations. The main difficulty in constructing a global PES is the choice of a suitable analytical function, which should properly reproduce the complicated PES topology at short and intermediate ranges, as well as for the anisotropic long-range interactions.

The aim of this study is to characterize low-lying structures and the stability of the H_5^+ cluster, and to provide a description of the $H_3^+ \dots H_2$ interaction at

intermediate and long intermolecular distances. For this purpose, first we performed high-level ab initio calculations using the QCISD(T) method. We report here theoretical predictions of the structures and energies of ten low-lying conformers of H_3^+ , as well as a series of QCISD(T) computations for various intermolecular distances and relative orientations of H_3^+ and H_2 in their equilibrium geometries. Second, we derived an analytical potential function using a first-order diatomics-in-molecule (DIM) perturbation approach in order to describe the $\text{H}_3^+ \dots \text{H}_2$ short-range interaction.

2 Ab initio calculations

2.1 Computational methods

Ab initio calculations were performed using the Gaussian 98 package [13]. The geometries of the H_3^+ stationary points were optimized at the QCISD(T) level of correlation treatment using cc-pVQZ, Dunning's quadruple-zeta correlation-consistent basis set. Vibrational frequency calculations were carried out at the same level of theory and were used to characterize the stationary points and to compute zero-point vibrational and dissociation energies of H_3^+ .

The accuracy of the present approaches for H_3^+ and H_2 monomers is indicated in Table 1, where the theoretical predictions of the QCISD(T)/cc-pVQZ calculations are compared with experimental data or best theoretical values available from literature [14–17]. Vibrational frequencies are given in the harmonic approximation whenever possible. Anharmonic and scaled frequency values are given in parentheses and brackets, respectively. For our ab initio calculations the frequencies are scaled by 0.9538 as recommended [18]. The present calculations reproduce the properties of the monomers very well. The geometric parameters are reproduced within 0.004 Å. The errors in the frequencies with respect to the reference values amount to only about 3 cm^{-1} for the harmonic frequencies of H_2 and to around 110 and 120 cm^{-1} for H_3^+ symmetric and asymmetric modes, respectively.

2.2 Structures and energetics of H_3^+

The geometry of H_3^+ is characterized using Cartesian coordinates. For comparison with previous calculations [3] we use only the following five coordinates: R_1 , R_2 are the H—H bond lengths in the H_3^+ monomer and α is the

angle between them, P is the H—H bond length in the H_2 monomer, and D is the intermolecular distance of one H atom of H_3^+ to the center of mass to H_2 for C_{2v} , D_{2d} and D_{2h} symmetries, as shown in Fig. 1. For different symmetries D is the intermolecular distance between the centers of mass of H_3^+ and H_2 (Fig. 2).

The results of the QCISD(T)/cc-pVQZ calculations for the optimized structures are summarized in Table 2 and depicted in Fig. 2. The present ab initio calculations reproduce all ten stationary points predicted by Yamaguchi et al. [3] (we keep the designation introduced by these authors), although they predict much lower electronic energies and introduce some changes in the energy order of the conformers. They keep the energy separation of 0.006 au between the four low-lying structures 1–4 and the other six. For the first four conformers, the correspondence between the present and previous ab initio results is remarkable, in particular, for the energy differences of the $1-C_{2v}$ – $2-D_{2d}$ and $3-C_{2v}$ – $4-D_{2h}$ structures, which represent the barriers for the proton transfer between two moieties in the planar and nonplanar conformations. In contrast, the relative order within the second group of structures, from 5 to 10, is different in our calculations. They predict a lower relative energy for the $9-C_s$ structure and higher one for the $6-C_{2v}$ one. Comparing these optimized geometries with the optimized geometries from full CI/DZP calculations [3], we should notice that D is greater in our calculations for the four lower-lying conformers and is shorter for the higher-lying conformers, i.e. $9-C_s$, $10-C_{3v}$, $7-C_{2v}$, etc.

The character of the stationary points, as well as the corresponding harmonic vibrational frequencies, were established through Hessian analysis. According to our QCISD(T)/cc-pVQZ calculations, the $1-C_{2v}$ structure is the energetically lowest stationary point and is the only true minimum among the ten stationary points. The numbers of imaginary frequencies for the other structures are 1 for $2-D_{2d}$, $3-C_{2v}$ and $5-C_{2v}$, 2 for $4-D_{2h}$, $6-C_{2v}$, $7-C_{2v}$ and $9-C_s$, 3 for $8-C_{2v}$, and 4 for the $10-C_{3v}$.

The results of the ab initio calculations on the vibrational frequencies of the $1-C_{2v}$ conformer of the H_3^+ complex are presented in Table 3 for comparison with the experimental data of Okumura et al. [2]. The values in parentheses refer to scaled ab initio frequencies. Using the scaling procedure, we get excellent agreement with the experimental data. Our estimates lie $(3928-3910) = 18 \text{ cm}^{-1}$ and $(3532-3500) = 32 \text{ cm}^{-1}$ above and below the assigned fundamentals of Okumura et al. [2]. Our estimates for ω_3 and ω_4 in H_3^+ are much lower than the corresponding degenerate asymmetric stretch-

Table 1. Equilibrium geometries, energies and frequencies of the H_3^+ and H_2 monomers calculated by the QCISD(T)/cc-pVQZ method compared with the best available experimental and/or

theoretical values. The frequencies (ω) given in *parentheses* refer to anharmonic transition frequencies. Scaled ab initio frequencies are given in *brackets*

Monomer	Method	Energy (au)	R_{HH} (Å)	ω (cm^{-1})
H_3^+	Experiment or theory	–1.343835 [14]	0.8770 [15]	(3175–3188) [14] (2522) [15]
	QCISD(T)/cc-pVQZ	–1.343110	0.8737	3437 [3279] 2772 [2644]
H_2	Experiment or theory	–1.174475 [16]	0.7415 [16]	4401 (4161) [17] –
	QCISD(T)/cc-pVQZ	–1.173797	0.7419	4404 [4201] –

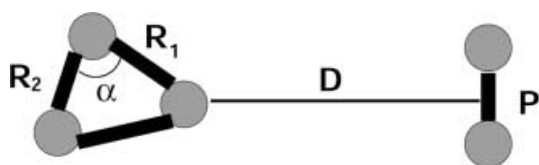


Fig. 1. Schematic representation of coordinates for the H_5^+ cluster

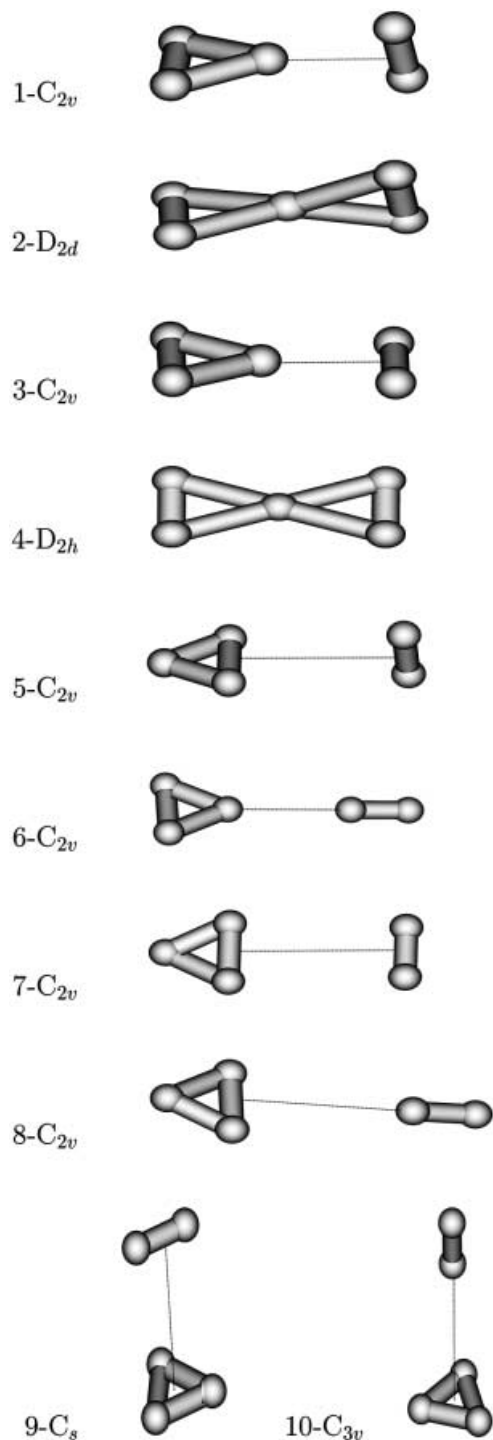


Fig. 2. Structures of the ten stationary points on the H_5^+ surface as predicted by ab initio calculations and the first-order diatomic-in-molecule perturbation theory model. The distances are in angstroms (see Tables 2, 5)

ing frequency of the H_3^+ molecule at 2522 cm^{-1} , but not to the same extent as the previous calculations [3].

This analysis as well as previous studies indicate that H_5^+ forms a weakly bound ion cluster with only minor changes in the H_3^+ and H_2 geometries. For this reason we performed a series of QCISD(T)/cc-pVQZ calculations for various intermolecular distances and relative orientations of H_3^+ and H_2 to give a description of the most important intermolecular interactions between H_3^+ and H_2 . We chose relative orientations for the H_3^+ and H_2 monomers according to the ten equilibrium conformers of H_5^+ . We performed calculations for the 1- C_{2v} , 3- C_{2v} , 5- C_{2v} , 7- C_{2v} , 9- C_s , 6- C_{2v} , 8- C_{2v} and 10- C_{3v} configurations keeping H_3^+ and H_2 in their equilibrium geometries and varying the distance between their centers of mass R , from 1.5 to 10 Å. The equilibrium geometries for H_3^+ and H_2 are taken from Table 1 according to our calculations. The results are presented in Fig. 3. We can notice the importance of the long-range electrostatic interactions for the different configurations. Among them the dominant ones are the charge-induced dipole(H_2), U_4 term

$$U_4 = -\left[\frac{1}{2}\alpha + \frac{1}{3}(\alpha_{\parallel} - \alpha_{\perp})P_2(\cos\theta)\right]/R^4$$

and the charge-(H_2) quadrupole, U_3 term

$$U_3 = Q_{H_2}P_2(\cos\theta)/R^3,$$

where θ is the angle between R and the H_2 bond, α , α_{\parallel} and α_{\perp} are the polarizabilities of the H_2 molecule, and Q_{H_2} is its quadrupole moment.

Both the U_4 and U_3 terms are attractive for the 1, 3, 5, 7 and 9 cases and in contrast to cases 6, 8 and 10 the charge-quadrupole term is repulsive. Consequently one expects completely different behavior for the curves of the previous two cases (Fig. 3). Evidently, attractive forces are stronger when H_2 approaches a corner of H_3^+ , (cases 1, 3 and 6) than a side (cases 5, 7 and 8) of the H_3^+ triangle. By comparing with the Hartree-Fock interaction energies given by Ahlrichs [5], we note that for the isomeric structures 1, 3, 5 and 7 the stabilization energies are of the same order but we get significant differences for cases 9, 6, 8 and 10. For these structures Ahlrichs predicted binding energies 1 order of magnitude smaller than in our calculations. Particularly, for the isomeric structure 9 a very shallow potential curve was predicted and for case 10 a repulsive curve. In contrast, we found that for these structures the short-range forces of chemical binding are not very small and are considerable for case 9.

Finally, the dissociation energy of H_5^+ to $H_3^+ + H_2$ is reported in Table 4. Our predictions for D_e , D_0 and ΔH° based on the QCISD(T)/cc-pVQZ calculations are compared with the data of different experimental [19–25] and theoretical [3, 7, 9, 10, 26] studies. To calculate vibrational zero-point energy corrections, both scaled and unscaled harmonic frequencies can be used. The latter values of D_0 are given in parentheses. Temperature corrections should not included, since a temperature of 298.15 K is close to the experimental values for H_5^+ (250–330 K, as established from the van't Hoff plots [24]). The enthalpy values, presented in brackets, are

Table 2. Geometries and energies for ten stationary points on the H_5^+ surface as predicted by ab initio QCISD(T)/cc-pVQZ calculations

Conformer	Energy (au)	Internal coordinates				
		R_1 (Å)	R_2 (Å)	α (deg)	D (Å)	P (Å)
1- C_{2v}	-2.530509	0.97704	0.81266	65.4	1.29177	0.76620
2- D_{2d}	-2.530217	1.12502	0.78487	69.6	1.05436	0.78487
3- C_{2v}	-2.530074	0.97008	0.81405	65.2	1.31711	0.76444
4- D_{2h}	-2.529680	1.12726	0.78385	69.7	1.05694	0.78385
5- C_{2v}	-2.523476	0.87043	0.87236	60.1	2.05752	0.74974
7- C_{2v}	-2.522890	0.86971	0.87222	60.1	2.10108	0.74874
9- C_s	-2.520616	0.87119	0.87119	60.0	2.50385	0.74556
6- C_{2v}	-2.520034	0.88870	0.85849	61.1	1.59985	0.74571
8- C_{2v}	-2.518374	0.87351	0.87345	60.0	2.15673	0.74319
10- C_{3v}	-2.517594	0.87312	0.87312	60.0	2.52917	0.74195

Table 3. Experimental and theoretical frequencies (cm^{-1}) for the monomers in H_5^+ (conformer 1- C_{2v}). The scaled values in *parentheses* are from Ref. [3] and those in *brackets* are from our calculations

Normal mode	Experiment [2]	Full CI/DZP [3]	QCISD(T)/cc-pVQZ
H_2 stretch (ω_1)	3910	4198 (3844)	4118 [3928]
H_3^+ symmetric stretch (ω_2)	3532	3824 (3439)	3670 [3500]
H_3^+ asymmetric stretch (ω_3)	—	2043 (1746)	2134 [2035]
H_3^+ symmetric stretch (ω_4)	—	1746 (1449)	1840 [1755]

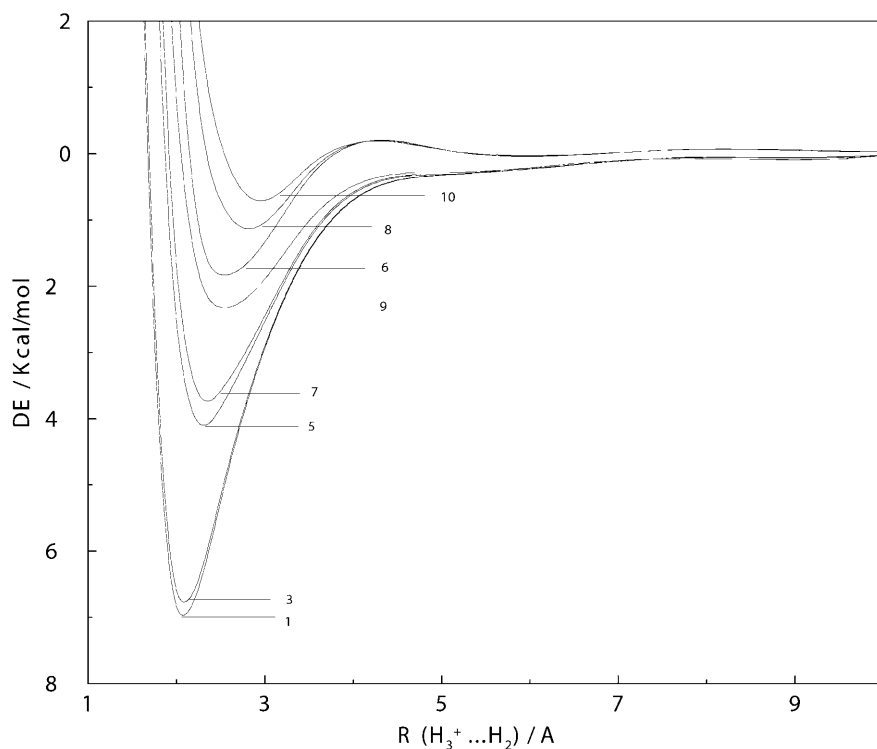


Fig. 3. Interaction energy for $H_3^+ \dots H_2$ (kcal/mol). The relative orientations for the two monomers are chosen from the ten conformers of H_5^+ (Fig. 2). R is the intermolecular distance connecting the centers of mass of the H_3^+ and H_2 monomers

corrected to 153 K for comparison with other calculations. Our estimate is in very good agreement with experimental data and recent G2(MP2) level calculations [9].

3 DIM PT1 interaction potential for H_5^+

3.1 Derivation of an analytical potential

The diatomics-in-molecule (DIM) approach provides an attractive way to describe the PES of H_n^+ clusters.

Indeed, the H_3^+ and H_3 molecules were the second systems (after H_2O) treated by DIM by its founders [27], who later considered H_n^+ clusters as well [28]. It was demonstrated [27, 29] that even the simplest DIM formulation, which implements the minimum basis set and neglects the overlap of atomic functions, gives quite reasonable results for the H_3 and H_3^+ molecules. Later, modified versions of the DIM method were used to calculate multivalued [30] and reactive [31] PESs. Very recent work by Aguado and coworkers [32, 33], where Ellison's DIM scheme was used to fit high-quality ab initio calculations on H_3^+ , demonstrated that only a

Table 4. Theoretical and experimental dissociation energies and enthalpies (kcal/mol) for H_3^+ . The values in *parentheses* are for unscaled harmonic frequencies; The values in *brackets* are for enthalpies corrected to 153 K

Experiment or theory	D_e	ΔZPE	D_0	$-\Delta H_T^0$
Arifov et al. (1971) [19]				5.1 ± 1.2
Bennet and Field (1972) [20]				9.7
Johnsen et al. (1976) [27]				8.1 ± 0.1
Elford (1983) [22]				5.8 ± 1.2
Beuhler et al. (1983) [23]				6.6 ± 0.3
Hiraoka (1987) [24]				6.9 ± 0.3
Hiraoka and Mori (1989) [25]				7.0 ± 0.1
SCF/DZ – Yamaguchi et al. (1983) [6]	3.35			
CI – Yamaguchi et al. (1987) [3]	8.34	2.89	5.45	
DQMC – Pang (1994) [26]			5.3	
DFT – Stich et al. (1997) [7]			14.5	
G2(MP2) – Ignacio and Yamabe (1998) [9]	8.90			[6.20]
MP4/CCSD(T) – Barbatti et al. (2000) [10]	7.84/7.72			[6.91]
QCISD(T)/cc-pVQZ – this work	8.54	2.64 (2.77)	5.90 (5.76)	7.25 [6.96]

small correction to the three-body (3B) interaction is needed to bring the resulting PES into agreement with experimental data and other available potentials [34–36]. In addition, the fragment nature of the DIM PT1 method makes easy the extension of the model to larger $\text{H}_3^+ \dots (\text{H}_2)_n$ clusters.

For the present purpose, we ought to formulate the simplest analytical DIM-based model and test its ability to represent the H_3^+ PES. One candidate is a first-order DIM perturbation theory (DIM PT1) which allows the determination (to a first-order approximation) of the interaction potential from the knowledge of (unperturbed) electronic wave functions of the monomers [37–42].

Previous and the present ab initio results indicate that the H_3^+ cluster ion could be considered as consisting of H_3^+ and H_2 moieties relatively weakly bound with each other. We also assume that its ground state arises from the interaction of two moieties in their ground singlet states and ignore the contributions from all other electronic configurations.

An appropriate representation of its total DIM Hamiltonian is therefore

$$\hat{H} = \sum_{i=1}^3 \sum_{k=1}^{i-1} \hat{H}_{ik} + \hat{H}_{ab} + \sum_{i=1}^3 \sum_{m=a,b} \hat{H}_{im} - 3 \sum_{i=1}^3 \hat{H}_i - 3 \sum_{m=a,b} \hat{H}_m . \quad (1)$$

The following convention is used: hydrogen atoms with $i = 1 - 3$ belong to H_3 , while $m = a, b$ for the H_2 moiety, \hat{H}_{ik} are for the Hamiltonian of a diatomic fragment composed from i th and k th atoms and \hat{H}_i denotes the atomic Hamiltonian.

From the zero-order approximation for infinitely separated moieties, we have

$$\hat{H}_0 = \hat{H}_{H_3} + \hat{H}_{H_2} , \quad (2)$$

with

$$\hat{H}_{H_3} = \sum_{i=1}^3 \sum_{k=1}^{i-1} \hat{H}_{ik} - \sum_{i=1}^3 \hat{H}_i , \quad (3)$$

and

$$\hat{H}_{H_2} = \hat{H}_{ab} - \hat{H}_a . \quad (4)$$

For the perturbation term we get $\hat{V} = \hat{H} - \hat{H}_0$.

In order to solve the Schrödinger equation for the unperturbed Hamiltonian \hat{H}_0 (Eq.2), polyatomic basis functions (PBF) should be introduced [43]. We define PBFs as independent products of atomic functions located on each site of the system. Following Ellison et al. [27], we use a minimal PBF basis consisting of two functions, $|\alpha\rangle_i$, and $|\beta\rangle_i$, describing the spin state of the hydrogen atom located at the i th site and one function, $|0\rangle_i$ which indicates that site i is occupied by the proton. This PBF set is considered as orthonormal [27].

The solution of the DIM problem for H_2 is trivial. It gives the valence bond singlet function

$$\phi_2 = (|\alpha\rangle_a |\beta\rangle_b - |\beta\rangle_a |\alpha\rangle_b) / \sqrt{2} \quad (5)$$

as the eigenvector and the ground singlet $^1\Sigma_g^+$ state, $S_{ab} = S(R_{ab})$ of H_2 as the eigenvalue. The DIM problem for H_3^+ is described in detail in Refs. [27, 29, 32]. Using the basis set composed of functions (Eq. 5) for (i, j) , (i, k) and (k, j) pairs of hydrogen atoms multiplied by the $|0\rangle$ function located at sites k, j and i , respectively, it is easy to evaluate the corresponding 3×3 matrix for the DIM Hamiltonian (Eq. 3). Its diagonalization gives the ground-state energy E_3 of the H_3^+ moiety as a function of the R_{ij} , R_{ik} and R_{kj} distances and the eigenvector ϕ_3 as an expansion over these functions, with the coefficients C_i depending on the same variables [27, 29, 32]. The squared coefficient C_i represents the probability of finding the proton on site i , or the partial charge of the hydrogen atom at this site.

To a first-order approximation, the interaction PES is given by

$$U_{\text{int}} = \langle \phi_2 \phi_3 | \hat{V} | \phi_2 \phi_3 \rangle . \quad (6)$$

Both ϕ_2 and ϕ_3 are expanded over the products of the atomic wave functions and \hat{V} is expressed as the sum of diatomic and atomic Hamiltonians. By applying the procedure pioneered by Ellison et al. [27] one obtains after analytical calculations

$$U_{\text{int}} = \frac{1}{2} \sum_{i=1}^3 C_i^2 \times \sum_{m=a,b} \left[(G_{im} + U_{im}) + \frac{1}{2} \sum_{l=1}^3 (1 - \delta_{il})(3T_{lm} + S_{lm}) \right]. \quad (7)$$

Here G_{im} , U_{im} and T_{lm} , S_{lm} are the energies of the H_2^+ ion in the ${}^2\Sigma_g^+$ and ${}^2\Sigma_u^+$ states and the energies of the H_2 molecule in the ${}^3\Sigma_u^+$ and ${}^1\Sigma_g^+$ states, respectively, as functions of the R_{im} distances between the i and m hydrogen atoms.

The first and second sums run over the sites of the H_3^+ and H_2 moieties, respectively. The first term in the brackets describes the interaction of the proton located on site i with the atoms of the H_2 moiety, while the second term corresponds to the interaction of the remaining part of H_3^+ (i.e., H_2 molecule) with the H_2 moiety. The C_i coefficients weight individual interactions according to the probability of finding the proton on site i . The final form of the H_3^+ DIM PT1 PES is

$$E = E_3 + S_{ab} + U_{\text{int}}, \quad (8)$$

where E_3 is the ground-state energy of H_3^+ as a function of the three interatomic distances, $S_{ab} = S(R_{ab})$ is the ground singlet ${}^1\Sigma_g^+$ state of H_2 and U_{int} is the interaction term as is given by Eq. (7).

3.2 Comparison of the DIM PT1 model and ab initio calculations

For implementing the DIM PT1 approach (Eq. 8) for H_3^+ we use the H_2 and H_2^+ potentials from Refs. [32, 44, 45, 46]. For the H_3^+ moiety, both the standard DIM approach [27, 29] and the DIM/3B approach described in Ref. [32] were implemented. The 3B correction introduced in the latter does not affect the interaction PES (Eq. 7), keeps the C_i coefficients unchanged, but improves the energy E_3 and its dependence on internal coordinates. As a result, the DIM method provides reasonable results although markedly overestimates the H_3^+ bond length, while the 3B correction brings the results in complete accord with experimental data.

We summarize the optimized geometries and energies of the stationary points on the DIM PT1 PES in Table 5 and Fig. 2. Surprisingly, this simple model is able to reproduce exactly the same set of stationary points with the same symmetry as the ab initio methodology. This shows that the analytical representation of the potential function provided by the model is topologically correct. However, there is no quantitative agreement between the model and ab initio results. Indeed, the DIM PT1 model tends to give much lower electronic energies and does not follow the order of conformers established in higher-level ab initio calculations. It predicts the lowest energy for the 9- C_s conformer, while the ground state 1- C_{2v} one appears to be only sixth in the dense manifold of other structures. In addition, in contrast to the ab initio calculations, the model does not give the prominent energy spacing between various conformers. The energies of eight structures fall within a gap of around 0.001 au and only the 2- D_{2d} and 4- D_{2h} structures have much higher energy, however, this is a limitation of the model itself. These structures represent the saddle points for the proton transfer, when the proton is situated in the middle of two hydrogen molecules. In the present diabatic formulation, the saddle points correspond to the crossing seam of two DIM PT1 surfaces in which the proton is explicitly assigned to one or another hydrogen molecule. This is the reason for artificially too high barriers for proton transfer (the energies and geometries of the 2- D_{2d} and 4- D_{2h} saddle points quoted in Table 5 were determined not by a global search, but by energy minimization along the crossing seam). To describe the adiabatic PESs, evaluation of diabatic coupling between two PESs is needed. Further, there is a huge difference in the locations of stationary points. The somewhat longer internuclear distances in the H_3^+ moiety reflect the deficiency of DIM, while the strong overestimation of the interfragment distance D means that the DIM PT1 model tends to underestimate the interaction between the moieties. DIM/3B correction does not influence the results a lot, giving only a shift in energy and the geometry of H_3^+ . It amounts, for instance, to -2.521482 au and $R_1 = R_2 = 0.8731$ Å for the 9- C_s conformer. It is worth noting that the DIM PT1 results agree better with SCF/DZ calculations than with our QCISD(T) values. For example, SCF/DZ calculation predicts [3] an energy of -2.407823 au and 1.7510 Å for the interfragment distance D for the 1- C_{2v} conformer.

Table 5. Geometries and energies for ten stationary points on the H_3^+ surface as predicted by the first-order diatomics-in-molecule perturbation theory (DIM PT1) model

Conformer	Energy (au)	Internal coordinates				
		R_1 (Å)	R_2 (Å)	α (deg)	D (Å)	P (Å)
9- C_s	-2.5323036	0.92237	0.92237	60.0	3.01190	0.74174
7- C_{2v}	-2.5320165	0.92308	0.92173	59.9	2.90201	0.74179
5- C_{2v}	-2.5319935	0.92294	0.92174	59.9	2.94641	0.74177
10- C_{3v}	-2.5318808	0.92239	0.92239	60.0	2.89808	0.74113
3- C_{2v}	-2.5316969	0.92135	0.92272	59.9	2.82973	0.74177
1- C_{2v}	-2.5316962	0.92134	0.92272	59.9	2.82875	0.74177
8- C_{2v}	-2.5316097	0.92222	0.92222	60.0	2.82386	0.74116
6- C_{2v}	-2.5313646	0.92151	0.92267	59.9	2.68014	0.74128
2- D_{2d}	-2.4082317	1.35126	0.81862	72.4	1.28778	0.81862
4- D_{2h}	-2.4081957	1.35235	0.81843	72.4	1.28895	0.81843

The harmonic vibrational frequencies for the $1-C_{2v}$ minimum structure of H_5^+ calculated within the DIM PT1 model and the QCISD(T)/cc-pVQZ methodology are compared with the results of full CI/DZ and SCF/DZ calculations from Ref. [3] in Table 6. The frequencies evaluated using the DIM PT1 model are in better accord with the SCF and CI results in the double-zeta basis (note that CI/DZ calculations also gave one imaginary frequency). However, the DIM PT1 model predicts too small shifts of the frequencies corresponding to the H_3^+ and H_2 monomers in the cluster and too low frequencies of intermolecular modes. In agreement with previous observations, this indicates the underestimation of intermolecular interaction within the model. Further, as should be expected, the DIM PT1 model predicts a very low binding energy (2.93 kcal/mol for DIM/3B PT1) that is closer to the estimates of SCF/DZ calculations (Table 4). The quantitative failure of this approach indicates the importance of the correct treatment of the long-range electrostatic interactions, first of all the charge-induced dipole and charge-quadrupole terms. It should be noted that inclusion of such terms in the functional form means that structures such as $1-C_{2v}$ are expected to be more attractive (see Sect. 2.2). An estimate of the contribution of the charge-induced dipole and charge-quadrupole interactions to the binding energy for the $1-C_{2v}$ configuration is about 3 kcal/mol (the values for the parameters are taken from Refs. [5, 47]).

4 Conclusions

The equilibrium structures, the features of the intermolecular interaction at intermediate and long distances and the stability of the H_5^+ cluster were investigated using a high-level ab initio method. The QCISD(T)/cc-pVQZ calculations, the most accurate to date for all conformers of the H_5^+ cluster, are in good accord with available experimental data.

An analytical description of the PES was attempted by means of DIM PT1 for intermolecular interactions. The simplest version of the DIM PT1 model, parameterized by the true diatomic potentials of H_2 and H_2^+ , was implemented to characterize the symmetries, geometries and energies of H_5^+ stationary points, as well

Table 6. Harmonic vibrational frequencies for the $1-C_{2v}$ conformer of H_5^+ (cm^{-1}) calculated at the QCISD(T)/cc-pVQZ, full CI/DZ [3] and SCF/DZ [3] levels of theory in comparison with DIM PT1 prediction. The ab initio frequencies are unscaled

Normal mode	QCISD(T)/cc-pVQZ	Full CI/DZ	SCF/DZ	DIM PT1
ω_1	4118 (A_1)	4209	4480	4400
ω_2	3670 (A_1)	3583	3712	3608
ω_3	2134 (B_2)	2602	2723	2455
ω_4	1840 (A_1)	2669	2779	2486
ω_5	1174 (B_1)	739	719	379
ω_6	868 (B_1)	515	534	184
ω_7	815 (B_2)	546	511	132
ω_8	502 (A_1)	462	442	102
ω_9	206 (A_2)	37i	104	46i

as vibrational frequencies and the dissociation energy. These data were compared with QCISD(T)/cc-pVQZ ab initio calculations. It was found that the model is able to reproduce the number and the symmetry of the stationary points, but not always their nature and relative energies. In general, the main drawback of the DIM PT1 model is the underestimation of the interaction strength between the fragments. Obviously, the main limitation of the DIM PT1 model is the inability to treat collective electrostatic interactions. For a proper treatment of the H_5^+ potential surface a minimum requirement should be a combination of the DIM PT1 model with long-range terms. Work in this direction is currently in progress.

Acknowledgements. We would like to thank V. Botella for informative discussions and A. van der Avoird for his valuable comments. Also we are grateful to O. Roncero, A. Aguado and M. Paniagua for providing their PES form for H_3^+ . Discussions with N. de Castro Faria, G. Jalbert, M. Nascimento and M. Barbatti are likewise appreciated. R.P. gratefully acknowledges funding by MEC, Spain (ref no. SB99 N0714831) and the European Commission (ref no. ERB FMRX-CT-96-0088). A.A.B. is also indebted to MEC for supporting his sabbatical stay at C.S.I.C. This work was supported by the DGICYT PB95-0071, HPRN-CT-1999-00005 and INTAS 97-31573 grants.

References

- Dawson PH, Thickner AW (1962) *J Chem Phys* 37: 672
- Okumura M, Yeh LI, Lee YT (1988) *J Chem Phys* 88: 79
- Yamaguchi Y, Gaw JF, Remington RB, Schaefer HF III (1987) *J Chem Phys* 86: 5072
- Nagashima U, Morokuma K, Tanaka H (1992) *J Phys Chem* 96: 4294
- Ahlrichs R (1975) *Theor Chim Acta* 39: 149
- Yamaguchi Y, Gaw JF, Schaefer HF III (1983) *J Chem Phys* 78: 4074
- Stich I, Marx D, Parrinello M, Terakura K (1997) *J Chem Phys* 107: 9482
- Farison M, Farison-Mazuy B, de Castro Faria NV, Chermentte H (1991) *Chem Phys Lett* 177: 45
- Ignacio EW, Yamabe S (1998) *Chem Phys Lett* 287: 563
- Barbatti M, Jalbert G, Nascimento MAC (2000) *J Chem Phys* 113: 4230
- Kirchner NJ, Bowers MT (1987) *J Phys Chem* 91: 2573
- (a) Talrose VL, Vinogradov PS, Larin IK (1979) In: Bowers MT (ed) *Gas phase ion chemistry*. Academic, New York, pp 305–347; (b) Douglass CH, Ringer G, Gentry WR (1982) *J Chem Phys* 76: 2423
- Frisch MJ, Trucks GW, Schlegel HB, Scuseria GE, Robb MA, Cheeseman JR, Zakrzewski VG, Montgomery JA Jr, Stratmann RE, Burant JC, Dapprich S, Millam JM, Daniels AD, Kudin KN, Strain MC, Farkas O, Tomasi J, Barone V, Cossi M, Cammi R, Mennucci B, Pomelli C, Adamo C, Clifford S, Ochterski J, Petersson GA, Ayala PY, Cui Q, Morokuma K, Malick DK, Rabuck AD, Raghavachari K, Foresman JB, Cioslowski J, Ortiz JV, Baboul AG, Stefanov BB, Liu G, Liashenko A, Piskorz P, Komaromi I, Gomperts R, Martin RL, Fox DJ, Keith T, Al-Laham MA, Peng CY, Nanayakkara A, Gonzalez C, Challacombe M, Gill PMW, Johnson B, Chen W, Wong MW, Andres JL, Gonzalez C, Head-Gordon M, Replogle ES, Pople JA *Gaussian 98*, revision A.7, Gaussian, Pittsburgh, Pa
- Röhse R, Kutzelnigg W, Jaquet R, Klopper W (1994) *J Chem Phys* 101: 2231
- Foster SC, McKellar ARW, Peterkin IR, Watson JKG, Pan FS, Crofton MW, Altman RS, Oka T (1986) *J Chem Phys* 84: 91
- Kolos W, Wolniewicz L (1968) *J Chem Phys* 49: 404

17. Huber KP, Herzberg G (1979) Constants of diatomic molecules. Van Nostrand Reinhold, New York
18. Scott AP, Radom L (1996) *J Phys Chem* 100: 16502
19. Arifov UA, Pozharov SL, Chernov IG, Mukhamediev ZA (1971) *High Energy Chem USSR* 5: 69
20. Bennet SL, Field FH (1972) *J Am Chem Soc* 94: 8669
21. Johnsen R, Huang C, Biondi MA (1976) *J Chem Phys* 65: 1539
22. Elford MT (1983) *J Chem Phys* 79: 5951
23. Beuhler RJ, Ehrenson S, Friedman L (1983) *J Chem Phys* 79: 5982
24. Hiraoka K (1987) *J Chem Phys* 87: 4048
25. Hiraoka K, Mori T (1989) *J Chem Phys* 91: 4821
26. Pang T (1994) *Chem Phys Lett* 228: 555
27. Ellison FO, Huff NT, Patel JC (1963) *J Am Chem Soc* 85: 3544
28. Pfeiffer GV, Huff NT, Greenawalt EM, Ellison FO (1967) *J Chem Phys* 46: 821
29. Tully JC (1971) *J Chem Phys* 54: 4297
30. Varandas AJC, Voronin AI (1995) *Mol Phys* 85: 497
31. Last I, Baer M (1981) *J Chem Phys* 75: 288
32. Aguado A, Roncero O, Tablero C, Sanz C, Paniagua M (2000) *J Chem Phys* 112: 1240
33. Sanz C, Roncero O, Tablero C, Aguado A, Paniagua M (2001) *J Chem Phys* 114: 2182
34. Prosimi R, Polyansky OL, Tennyson J (1997) *Chem Phys Lett* 273: 107
35. Polyansky OL, Prosimi R, Klopper W, Tennyson J (2000) *Mol Phys* 98: 261
36. Cencek W, Rychlewski J, Jaquet R, Kutzelnigg W (1998) *J Chem Phys* 108: 2831
37. Naumkin FY (1991) *Sov Phys Lebedev Inst Rep USA* 8: 27
38. Buchachenko AA, Stepanov NF (1996) *J Chem Phys* 104: 9913
39. Buchachenko AA, Stepanov NF (1997) *J Chem Phys* 106: 10134
40. Buchachenko AA, Stepanov NF (1998) *Russ J Phys Chem* 72: 69
41. Buchachenko AA, Stepanov NF, Grigorenko BL, Nemukhin AV (1999) *J Chem Phys* 111: 2470
42. Grigorenko BL, Moskovsky AA, Nemukhin AV (2000) *J Mol Struct (THEOCHEM)* 498: 47
43. Tully JC (1977) In: Segal GA (ed) *Semiempirical methods of electronic structure theory*. Plenum, New York pp 199, PART A
44. Kolos W, Wolniewicz L (1965) *J Chem Phys* 43: 2429
45. Bates DR, Ledsham K, Stewart AL (1953) *Philos Trans Lond R Soc A* 246: 215
46. Bishop DM, Wetmore RW (1973) *Mol Phys* 26: 145
47. Giese CF, Gentry WR (1974) *Phys Rev A* 10: 2156